Regular Article

PHYSICAL CHEMISTRY RESEARCH
Published by the
Iranian Chemical Society
www.physchemres.org
info@physchemres.org

Phys. Chem. Res., Vol. 8, No. 1, 111-124, March 2020
DOI: 10.22036/pcr.2019.203023.1680

Removal of Azo Dye Calcon Using Polyaniline Films Electrodeposited on SnO_2 Substrate

M. Ait Himi[a,*], S. El Ghachtouli[a,*], A. Amarray[a], Z. Zaroual[a], P. Bonnaillie[b] and M. Azzi[a]

[a]*Laboratoire Interface Matériaux Environnement, Faculté des Sciences Ain Chock, BP 5366 Maârif, Casablanca, Maroc*

[b]*DEN/DMN/SRMP, CEA Saclay, 91191 Gif-sur-Yvette, France*

(Received 26 September 2019, Accepted 4 December 2019)

In order to find simple, effective and economical methods for dye adsorption, the present work aims at studying the adsorption efficiency of an azo dye "Calcon'' by polyaniline (PA) films prepared by the electrochemical method. The characterization of these films by X-ray diffraction (XRD), scanning electron microscopy (SEM) and UV-Vis spectrophotometer shows an amorphous fibrillary structure for the PA electrodeposited films. To find the best conditions for adsorption of Calcon dye, the effect of pH, hydrogen peroxide, contact time and the initial Calcon concentration were studied. The experiments showed the possibility of increasing the adsorption capacity from 42% to 54% while pH changes from 9 to 3. This value increases to 98.6% by the addition of hydrogen peroxide. On the other hand, the effect of Calcon concentration was studied from 15 to 50 mg l^{-1}, the results indicated that the discoloration of Calcon dye decreases with the increase in dye concentration. However, kinetics and isotherm studies have shown that the adsorption reaction follows the pseudo-second-order model, the adsorption process follows the Langmuir isotherm model, and the PA electrodeposited has a monolayer adsorption capacity of 606mg/g which is considerably high compared to all polyaniline forms prepared chemically.

Keywords: Polyaniline (PA), Electrodeposition, Azo dye, Calcon, Adsorption

INTRODUCTION

Dyes are an abundant class of colored organic compounds that represent an increasing environmental danger [1]. Toxic dye waste in aquatic environments remains a real problem up to date. Synthetic dyes generally represent a complex aromatic molecular structure [2]. They are stable and therefore hard to biodegrade. Azo dyes play an important part in the textile dyeing process, presenting a wide range of colors and allowing a quick and better dying. As a consequence, the discoloration or removal of these compounds from the environment remains an important issue [3].

Due to their very large production and consumption, it is now very urgent to develop new processes of organic compound degradation, being non-toxic, low-cost efficient and able to eliminate these pollutants from contaminated water. Several treatment processes have been applied for the removal of dye from wastewater such as ion exchange [4], adsorption [5], precipitation [6], biodegradation [7], membrane filtration, coagulation, flocculation [8], *etc.* Adsorption is an eco-safety procedure of choice for the removal of dyes, and heavy metals from wastewater [9]. In the last few years, the development of new and effective adsorbents with high adsorption capacity, low toxicity and efficient separation has attracted great attention [10]. In this context, several efficient and selective adsorbent materials have been developed, such as the activated carbon [11], clay [12], bioadsorbents [13], agricultural waste [14,15] and polymers [16]. Conducting polymer materials are widely used in different fields of science and industry, as electrodes in rechargeable batteries, electrochromic displays, anti-corrosion coatings, electromagnetic interference shielding, sensors, separation membranes, *etc*. Polyaniline (PA) is one

*Corresponding authors. E-mail: mohamedathm@gmail.com; s.elghachtouli@gmail.com

of the most interesting conducting polymers due to its environmental stability [17]. The insoluble and infusible nature of PA hampers is used in various applications such as electrochemical devices including batteries, capacitors, electrochromic windows and displays, actuators, photovoltaic and light-emitting electrochemical cells [18]. Few studies were also carried out on the application of PA as an adsorbent of harmful organic dye molecules [19-21]. However, most of these studies use polyaniline in the powder form, which is generally chemically prepared and requires filtration steps after treatment. This can be avoided by immobilizing the polyaniline on substrates [22-24], or by using the electrochemical method for its elaboration. The chemical way of synthesis is rather simple and cheap in comparison with the electrochemical one. Hence, the electrochemical deposition of polyaniline is a more environmentally desirable method as compared to the chemical method. The electrochemical method has several advantages over chemical polymerization. Electrochemical polymerization of aniline proves to be particularly attractive for the reasons as follows: (i) the electrochemical method is more preferable when the polymer product is to be used as a polymer film electrode [25], thin layer sensor [26], or in microtechnology [27], (ii) the electrochemical way of the PA synthesis makes it possible to receive films with different thickness and morphology by a simple change in electrolysis conditions [28], electrolyte composition [29], pH, temperature, solvent, dopant ions used and nature of substrate [30], (iii) the electrochemically deposited films are homogenous and adhere strongly to the electrode surface on a large-area substrate [31,32], (iv) the electrochemical polymerization enables us to avoid by-products of the process implying that PA obtained in this way is pure, without any impurities.

In the present work, the PA thin film was electrochemically deposited on SnO_2 substrate coated glass electrode by cyclic voltammetry. The PA/SnO_2 obtained was characterized by XRD, SEM and UV-Vis. The main purpose of the present research is to study the ability of PA/SnO_2 electrodeposited films to remove Calcon dye from aqueous solutions in the batch system. The effects of different parameters such as the solution's pH, the initial dye concentration and the presence of hydrogen peroxide have been studied. Also, the kinetics and the isotherm adsorption model have been investigated.

EXPERIMENTAL

Chemical Compounds

Aniline (ACS reagent ≥ 99.5%) was distilled under reduced pressure and stored in the dark below 4 °C. H_2SO_4 (reagent grade, 95-98%), H_2O_2 (ACS reagent, 30%), HCl (ACS reagent, 37%), NaOH (reagent grade, 97%), and the Calcon dye were purchased from sigma Aldrich and were used without further purification. Stock solutions of the dyes were prepared using Millipore Milli-Q deionized water.

Electrochemical Synthesis

The electrochemical measurements were performed at room temperature using a potentiostat (type Voltalabpgz 301) controlled by the Voltamaster (version 4) software. The polymerization experiments were carried out in a classical electrochemical cell with three electrodes. The counter electrode was a platinum wire. The reference electrode was a saturated calomel electrode (SCE). All potential values mentioned in the text refer to this reference electrode. The working electrode is a glass plate covered with tin dioxide (SOLEMS, 15 mm × 60 mm). The SnO_2 substrates were cleaned using acetone in an ultrasonic bath for 10 min before use. The surface of the SnO_2 substrate was 3 cm^2. All measurements were performed at room temperature, in an ambient air.

Characterization

The spectroscopic experiments were carried out using on Shimadzu dual-beam spectrophotometer model UV-1800. The analysis of film was determined by XRD using a BRUKER D8 ADVANCE diffractometer with radiation (Kα (λ = 1.5456 Å) equipped with a curved position sensitive detection.

The morphology and the microstructure of the films were examined by scanning electron microscopy (SEM) with a FEG Gemini 15-25 from LEO at an emission voltage of 5 keV.

Interaction Studies

The PA thin film coated SnO_2 coated glass substrate was

immersed into Calcon dye solution (V = 10 ml) and stirred in darkness at room temperature. The pH of the solution was adjusted with a small aliquot of HCl or NaOH (1 M). After interactions, the thin layers were removed from the solution, rinsed with Milli-Q water and stocked for further characterizations. The solutions were afterward stocked in a refrigerator waiting to be analyzed.

The discoloration efficiency (%) of dye was calculated using the following formula:

$$R(\%) = \frac{A_0 - A}{A_0} \times 100$$

where A_0 is the initial absorbance measured at λ_{max} = 542 nm (at pH = 6), and A is the absorbance measured at λ_{max} = 542 nm at t (h).

RESULTS AND DISCUSSION

Electrochemical Synthesis of PA

The electro-polymerization of aniline was carried out on the SnO_2 coated glass substrate using cyclic voltammetry at 10 mV s^{-1}, between -0.6 and 1.4V *vs*. SCE for 15 scans in the solution of 0.5 M H_2SO_4 and the presence of 20 mM of aniline. The cyclic voltammograms are shown in Fig. 1.

During the first anodic scan (inset Fig. 1), a system appears at 1.1 V, the recording of the latter came along with the formation of a thin green film of polyaniline, showing that this first anodic peak corresponds to the polymerization reaction of aniline to polyaniline, and more precisely to pernigraniline form. Thus, during the return to potential, three peaks of reduction have been observed. The latter corresponds to the transition from one form of polyaniline to another. Pernigraniline formed underwent the first reduction at 0.3 V. According to the literature [33], this reduction is attributed to the partial degradation of the quinone form into hydroquinone. The deposited pernigraniline form is then reduced at -0.2 V in emerald form. The latter was reduced successively to -0.5V in the form of leucoemeraldine, which is then oxidized to emerald form [34].

After electrodeposition, the green thin films were rinsed with Milli-Q water and dried in ambient air. Samples can be electrodeposited and stocked before interaction experiments. In these conditions, the weight of the material electrodeposited on SnO_2 substrate is m = (0.3 ± 0.1) $\times 10^{-3}$ g and its thickness is e = (0.7 ± 0.1) µm. This was later evaluated with the reported density of PA (d = 1.4) [35].

XRD Analysis

Figure 2 shows XRD patterns obtained on the adherent deep green solid electrodeposited on the SnO_2 substrate (picture inset (Fig. 2). The XRD patterns of pure SnO_2 and PA/SnO_2 electrode are compared in Fig. 2. However, the peak at 2θ = 25.6° can be attributed to PA, it can be caused by periodicity perpendicular to the conjugated chain of PA [37]. The XRD pattern shows that the deposited PA/SnO_2 thin film is amorphous. Such amorphous behavior has been reported in the literature [36] for the chemical synthesis of PA.

UV-Vis Adsorption

Figure 3 represents the UV-Vis absorption spectra of electrodeposited PA film on the SnO_2 electrode while using solid support material. The absorption spectrum of PA shows three characteristic absorption peaks at 330, 432 and 890 nm. The absorption peak at 330 nm can be ascribed to the π→π* transition of the benzenoidrings, while the peaks at 432 and 890 nm can be attributed to the polaron-π* transition and the π-polaron transition, respectively. Furthermore, the peaks at 432 and 890 nm are related to the doping level and formation of polaron form as described in previous studies [38,39].

Morphology of PA Films

SEM was used to study the detailed surface morphology of the polymer film coated on the SnO_2 electrode. The morphology of PA/SnO_2 was uniformly fibrillar and highly porous as seen in Fig. 4. This property is interesting because several studies have shown that polyaniline nanofiber has a high potential in enhancing performance for the removal of contaminants from water [40,41].

Catalytic Performance of PA

It is conceived that higher affinity towards the exposed regions of amine and imine units contained in the ordered PA may increase the affinity of charge dyes thus resulting in efficient adsorption of molecules. Following this

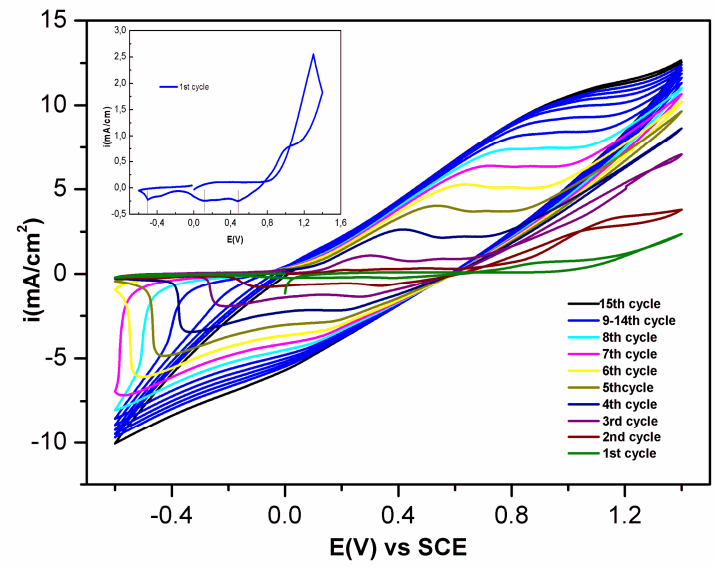

Fig. 1. Cyclic voltammograms of Aniline (20 mM) in H_2SO_4 (0.5 M), V = 10 mV s^{-1}.

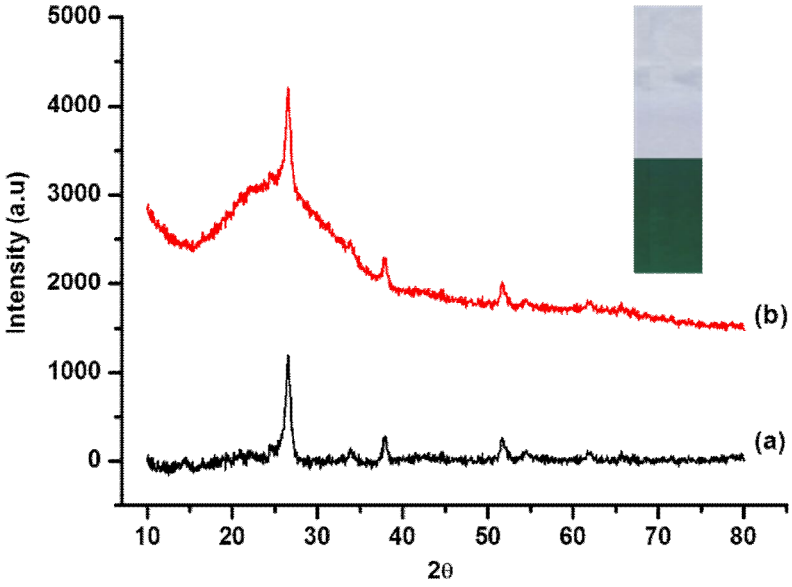

Fig. 2. XRD patterns of (a) SnO_2 substrate and (b) PA thin film electrodeposited on SnO_2 substrate. Inset: Image of PA thin film deposited on the SnO_2 substrate.

suggestion, the catalytic activity of the PA/SnO_2 electrode prepared was evaluated by oxidation of Calcon dye in an aqueous solution under different conditions.

Effect of initial pH. The molecular structure and the typical UV-Vis absorption spectrum of the initial Calcon dye solution at free pH (pH = 6) are presented in Fig. 5.

According to several works, the degradation of azo-dye strongly depends on the initial solution's pH. For this

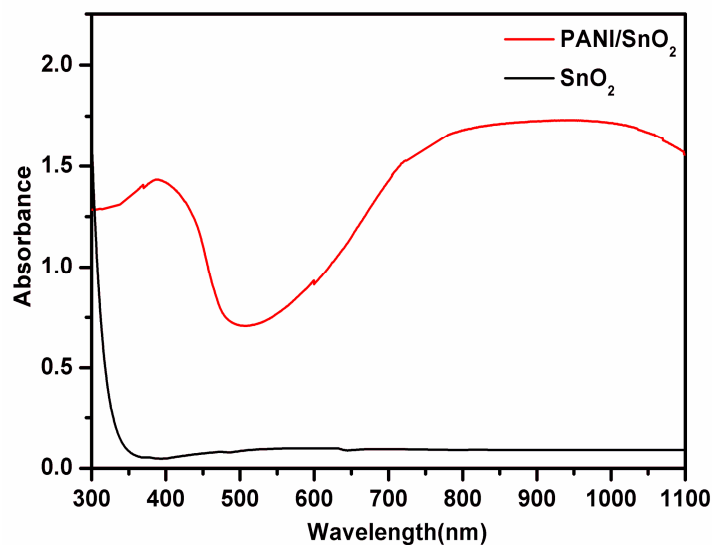

Fig. 3. UV-Vis spectra of electrodeposited PA/SnO_2.

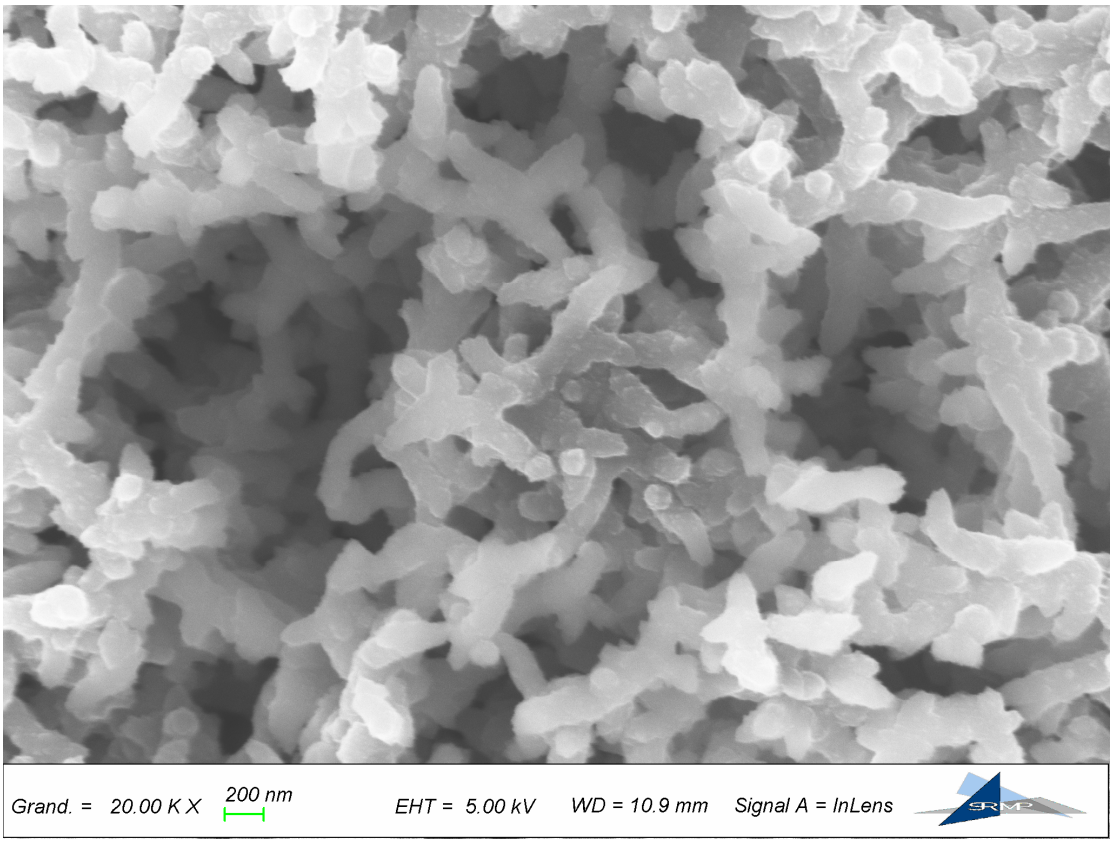

Fig. 4. SEM image of electrodeposited PA/SnO_2 films.

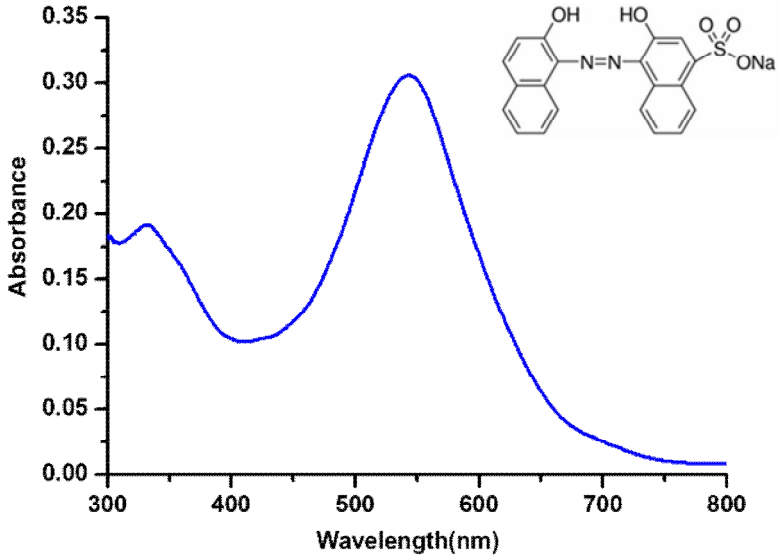

Fig. 5. Molecular structure and UV-Vis absorption spectrum of Calcon dye at free pH (pH = 6).

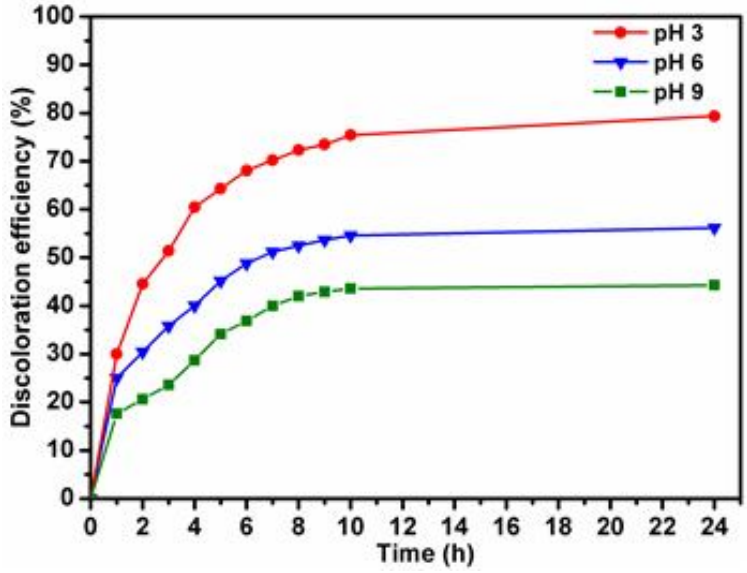

Fig. 6. Evolution with the time of discoloration efficiency of Calcon solution (15 mg l^{-1}) in interaction with a sample of PA/SnO_2 thin film at pH = 3, 6 and 9.

purpose, the PA/SnO_2 film prepared was put to interact with 20 ml of Calcon solution containing 15 mg l^{-1} at three initial pH values: 3, 6 and 9. Analogously, a similar measurement was made for the SnO_2 substrates without PA which showed no discoloration as expected. Figure 6 shows the influence of pH (3, 6 and 9) on the removal of Calcon dye from the aqueous solution with an initial concentration of 15 mg l^{-1}. However, the solution in interaction only with SnO_2 in the same condition remains purple without any modification of UV-Vis spectra. These results show the positive effect of PA/SnO_2 compared to SnO_2. The thin film of PA after interaction remains adherent and dark green without change.

As seen in Fig. 6, after 24 h, the degradation efficiencies of the Calcon dye from solution by PA/SnO_2 is 54 and 42% at pH = 6 and 9, respectively, which are considerably lower than those at pH = 3 (70%). This behavior can be explained by the variation of Calcon dye's structure at acidic pHs. Similar to all azo dyes, Calcon switches between two molecular structures depending on pH. In acidic aqueous solutions, the functional group of Calcon ($\equiv SO_3Na$) gets ionized to give ($\equiv SO_3^-$), so the dye is in an ionic form. The sulfonic groups ($\equiv SO_3^-$) on the Calcon dye, which apply electrostatic interactions with the positively charged dimine nitrogen of the doped PA film, are held responsible for fixing the dye. In alkaline aqueous solutions, the dissociation of the functional group of the dye would be inhibited, and therefore, no chemical interaction with the PA film would be expected [42]. The pH = 3 has been finally chosen for the rest of the experiments.

Effect of [H_2O_2]. The catalytic activity of PA/SnO_2 due to the removal of the Calcon dye solution was investigated in the presence of hydrogen peroxide (3×10^{-3} M) at pH = 3. As shown in Fig. 7, from the first hour of interaction between PA and solution, a discoloration efficiency of 53% was observed in the presence of H_2O_2 while only 30% was observed in the absence of H_2O_2. The discoloration efficiency continues to increase reaching 98.64% after 24 h of interaction. When we mixed the dye solutions with H_2O_2 and omitted PA/SnO_2 sample, only 10% of discoloration efficiency was observed.

The catalytic activity of the PA/SnO_2 in the presence of H_2O_2 at pH = 3 is adjacent to that reported for the Fenton-like reaction of H_2O_2 for the generation of free radical species [43]. A reaction mechanism implying free radical species can be suggested as:

$$(PA)_{ox} + H_2O_2 \rightarrow (PA)_{red} + HO_2^{\bullet} + H^+ \quad (1)$$

$$(Dye) + HO_2^{\bullet} \rightarrow (Dye)_{ox} \quad (2)$$

$$(PA)_{red} + H^+ \rightarrow (PA)_{ox} \quad (3)$$

The reduction of oxidized PA by H_2O_2 leads to the formation of $HO_2^{\bullet}$ radical species, Eq. (1). The generated radicals will attack the dye molecules, Eq. (2), causing discoloration of the solution. It is well documented that the conversion between EB and ES forms of PA can be occurred by protonation. Thus, the oxidized form of PA is obtained by protonation according to Eq.(3).

Effect of Calcon concentration. The effect of Calcon concentration was studied from 15 to 50 mg l^{-1} at pH = 3 in the presence of 3 mM of H_2O_2. The results are shown in Fig. 8.

Figure 8 shows that when the initial dye concentration is 15 mg l^{-1}, the treatment is effective at about 98.64% and the solution is completely discolored after 24 h. It seems that the discoloration of Calcon dye decreases quickly to 84.42%, 56.10%, 44.6% and 36.31% for 20, 30, 40 and 50 mg l^{-1}, respectively. Lower discoloration efficiency was obtained because of the saturation of the adsorption site of PA/SnO_2. At lower concentrations, all Calcon dye solutions could interact with the binding sites on the surface of PA/SnO_2 resulting in higher discoloration yields [39].

Kinetics Studies

In order to investigate the kinetics of Calcon's absorption on PA/SnO_2, pseudo-first-order and pseudo-second-order models were applied, as respectively shown in the linear forms (4) and (5) [44].

$$\ln(Q_e - Q_t) = \mathrm{Ln}\,(Q_e) - k_1/2.303\ t \quad (4)$$

$$t/Q_t = 1/(k_2 Q_e^2) + t/Q_e \quad (5)$$

Where Q_e and Q_t (mg g^{-1}) refer to the amounts of dye adsorbed per unit mass of the adsorbent respectively at equilibrium and at time t. k_1 (h^{-1}) is the rate constant of pseudo-first-order. k_2 (g mg^{-1} h^{-1}) is the rate constant of pseudo-second-order.

These models have been applied for 15 mg l^{-1} of Calcon at pH 3 and room temperature using PA/SnO_2. The data of both models are shown in Fig. 9. The constants and the correlation factor of both models are presented in Table 1.

The R^2 (0.9997) value of the pseudo-second-order model is close to 1 and higher than that in the pseudo-first-order model (0.94286). This shows that the reaction followed the pseudo-second-order model. Therefore, the reaction is controlled by chemisorption which involved valence forces through the exchange of electrons between Calcon and PA/SnO_2 [45].

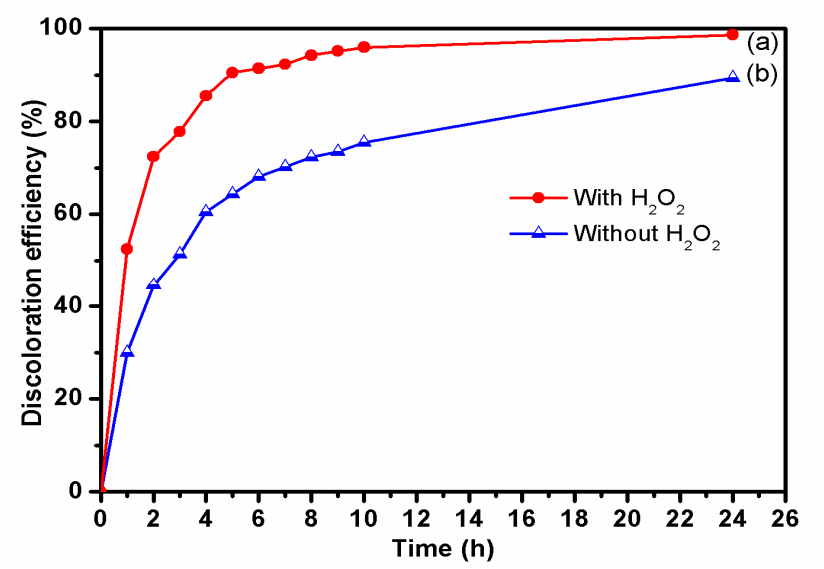

Fig. 7. Evolution with the time of discoloration efficiency of Calcon solution (15 mg l^{-1}) in interaction with a sample of PA/SnO_2 thin film at pH = 3, a) with H_2O_2 (3×10^{-3} M), b) without H_2O_2.

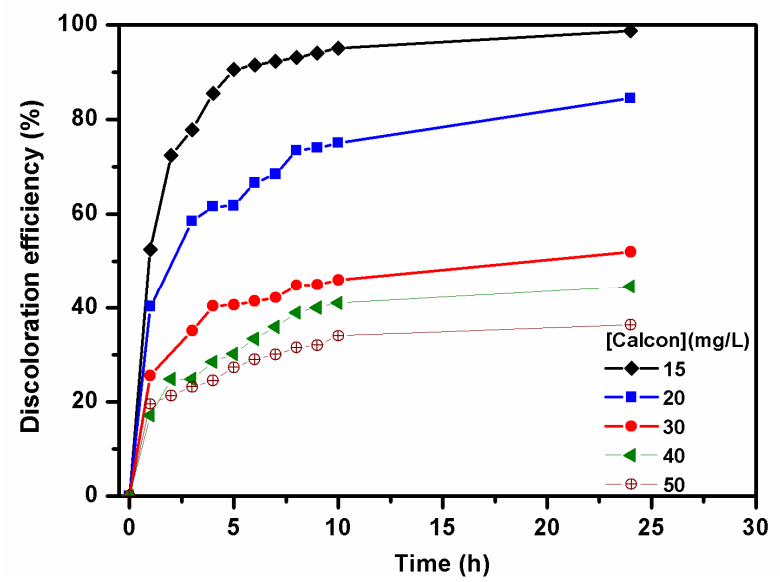

Fig. 8. Time evolution of discoloration efficiency of Calcon solution in interaction with a sample of PA/SnO_2 thin films at different concentrations, (pH = 3), and H_2O_2 (3×10^{-3} M).

Study of Isotherms

To understand the nature of adsorption equilibrium between Calcon dye and PA/SnO_2, the Langmuir, Freundlich and Temkin isotherm models were used. Their linear equations can be expressed by Eqs. (6), (7) and (8),

Langmuir: $C_e/Q_e = C_e/Q_0 + 1/(Q_0K_L)$ (6)

Freundlich: $\log Q_e = \log K_f + 1/n \log C_e$ (7)

Temkin: $Q_e = RT/b \ln A_T + RT/b \ln C_e$ (8)

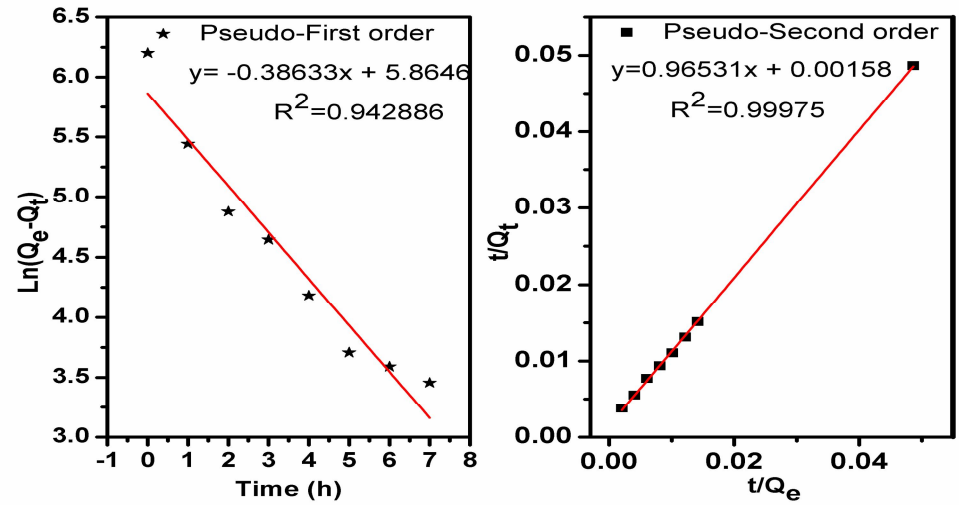

Fig. 9. Pseudo-first and pseudo-second-order graphs of Calcon adsorption on PA/SnO_2.

Table 1. Kinetic Parameters for the Adsorption of Calcon on PA/SnO_2

Pseudo-first order	k_1	Q_e	R^2
	(h^{-1})	(mg g^{-1})	
	0.8897	352.33	0.94286
Pseudo-second order	k_2	Q_e	R^2
	(g mg^{-1} h^{-1})	(mg g^{-1})	
	2.6036×10^{-3}	493.21	0.9997

where C_e = the equilibrium concentration of adsorbate (mg l^{-1}), Q_e = the amount of dye adsorbed per gram of the adsorbent at equilibrium (mg g^{-1}), Q_o = maximum monolayer coverage capacity (mg g^{-1}), K_L = Langmuir isotherm constant (l mg^{-1}), K_f (l mg^{-1}) and n = Freundlich isotherm constants, b = Temkin isotherm constant, A_T = Temkin isotherm equilibrium binding constant (l g^{-1}).

The linear plots of three isotherm models are presented in Figure 10. The values obtained by fitting data of three models are listed in Table 2.

The high value of the correlation coefficient (0.9986) of the Langmuir isotherm indicates the available application of this isotherm, which assumes that the adsorption energy is independent of calcon amount adsorbed on PA. The adsorption capacity of each active site is identical, and the availability of the adsorbate at a particular site imposes no impact on other sites [46]. These sites are homogeneously distributed over the surface of PA/SnO_2 and have the same affinity for adsorption of a mono molecular layer, so there is no interaction between adsorbed molecules [47]. This model also shows that PA/SnO_2 has a monolayer coverage ability of 606 mg g^{-1}. This value is very large compared to PA prepared by chemical means [48]. This is probably due to the good distribution of the mass on SnO_2 using the electrochemical way of PA's elaboration.

The essential features of the Langmuir isotherm may be expressed in terms of equilibrium parameter R_L, which is a dimensionless constant referred to as the separation factor

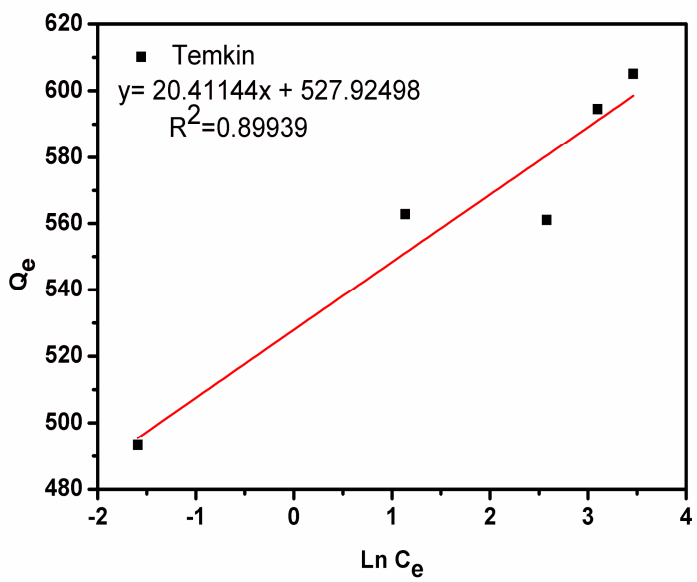

Fig. 10. The linear plot of Freundlich, Langmuir and Temkin isotherm models for the adsorption of Calcon dye in PA/SnO_2.

Table 2. Langmuir, Freundlich and Temkin Isotherm Model Constants and Correlation Coefficients for Adsorption Calcon dye in PA/SnO_2

Langmuir			Freundlich			Temkin		
Q_0	K_L	R^2	K_f	n	R^2	A_T	b	R^2
(mg g^{-1})	(l mg^{-1})		(l mg^{-1})			(l g^{-1})		
606	2.7591	0.99866	526.526	26.66	0.90516	1.7×10^{11}	121.32	0.8993

or equilibrium parameter [49]. This parameter can be expressed according to the following Eq. (9):

$$R_L = \frac{1}{1 + K_L C_0}$$

where the value of R_L indicates the type of isotherm: irreversible ($R_L = 0$), favorable ($0 < R_L < 1$), linear ($R_L = 1$), unfavorable ($R_L > 1$) [50], the value of R_L in the present work is in the range of 0-1 indicating a favorable adsorption of Calcon on PA/SnO_2. The Freundlich isotherm constant (n) represents the diversion of the adsorption process for $n = 1$, $n < 1$ and $n > 1$, the adsorption process will be performed *via* a linear, chemical, or physical mechanism, respectively [51]. On this work $n > 1$ indicating the adsorption process is performed via a physical mechanism.

CONCLUSIONS

The present work was dedicated to studying the efficiency of polyaniline films electrodeposited on the SnO_2 substrate to remove an azo dye "Calcon". First, the characterization by XRD, SEM, and UV-visible shows an amorphous structure of PA/SnO_2 electrodeposited. Afterward, it was demonstrated that the polyaniline prepared has an adsorption power up to 98.6% of Calcon.

The adsorption kinetic was well fitted to the pseudo-second-order model, and equilibrium data were favorably described by the Langmuir isotherm model. The adsorption process of azo dye by PA/SnO_2 is performed *via* a physical mechanism. We have found that the electrochemically prepared polyaniline has a very high monolayer adsorption capability; the capacity of 606 mg g^{-1} which is considerably high compared to all the forms of polyaniline prepared chemically.

REFERENCES

[1] Wang, J. C.; Lou, H. H.; Xu, Z. H.; Cui, C. X.; Li, Z. J.; Jiang, K.; Zhang, Y. P.; Qu, L. B.; Shi, W., Natural sunlight driven highly efficient photocatalysis for simultaneous degradation of rhodamine B and methyl orange using I/C codoped TiO_2 photocatalyst, *J. Hazard. Mater.* **2018**, *360*, 356-363. DOI: 10.1016/j.jhazmat.2018.08.008.

[2] Hayat, H.; Mahmood, Q.; Pervez, A.; Bhatti, Z. A.; Baig, S. A., Comparative decolorization of dyes in textile wastewater using biological and chemical treatment. *Sep. Purif. Technol.* **2015**, *154*, 149-153. DOI: 10.1016/j.seppur.2015.09.025.

[3] Bansal, P.; Singh, D.; Sud, D., Photocatalytic degradation of azo dye in aqueous TiO_2 suspension: Reaction pathway and identification of intermediates products by LC/MS. *Sep. Purif. Technol.* **2010**, *72*, 357-365. DOI: 10.1016/j.seppur.2010.03.005.

[4] Khan, M. I.; Akhtar, S.; Zafar, S.; Shaheen, A.; Khan, M. A.; Luque, R.; Rehman, A. Ur., Removal of congo red from aqueous solution by anion exchange membrane (EBTAC): Adsorption kinetics and themodynamics. *Materials.* **2015**, *8*, 4147-4161. DOI: 10.3390/ma8074147.

[5] Foroutan, R.; Mohammadi, R.; Farjadfard, S.; Esmaeili, H.; Saberi, M.; Sahebi, S., Characteristics and performance of Cd, Ni and Pb bio-adsorption using callinectes sapidus biomass : real wastewater treatment, *Environ. Sci. Pollut. Res.* **2019**, *26*, 6336-6347. DOI: 10.1007/s11356-018-04108-8.

[6] Zodi, S.; Merzouk, B.; Potier, O.; Lapicque, F.; Leclerc, J. P., Direct red 81 dye removal by a continuous flow electrocoagulation/flotation reactor. *Sep. Purif. Technol.* **2013**, *108*, 215-222. DOI: 10.1016/j.seppur.2013.01.052.

[7] Duarte Baumer, J.; Valério, A.; de Souza, S. M. A. G. U.; Erzinger, G. S.; Furigo, A.; de Souza, A. A. U., Toxicity of enzymatically decolored textile dyes solution by horseradish peroxidase. *J. Hazard. Mater.* **2018**, *360*, 82-88. DOI: 10.1016/j.jhazmat.2018.07.102.

[8] Wakrim, A.; Byoud, F.; El Ghachtouli, S.; Jamal Eddine, J.; Azzi-Martin, L.; Azzi, M., Discoloration study of azo dye solution using the fenton process, *Eur. J. Eng. Res. Sci.* **2018**, *3*, 75-80. DOI: 10.24018/ejers.2018.3.10.915.

[9] Kausar, A.; Iqbal, M.; Javed, A.; Aftab, K.; Nazli, Z. I. H.; Bhatti, H. N.; Nouren, S., Dyes adsorption using clay and modified clay: A review. *J. Mol. Liq.* **2018**, *256*, 395-407. DOI: 10.1016/j.molliq.2018.02.034.

[10] Tamjidi, S.; Esmaeili, H.; Kamyab, M. B., Application of magnetic adsorbents for removal of heavy metals from wastewater: a review study, *Mater. Res. Express.* **2019**, *6*, 102004. DOI: 10.1088/2053-1591/ab3ffb.

[11] Mousavi, S. M.; Hashemi, S. A.; Amani, A. M.; Esmaeili, H.; Ghasemi, Y.; Babapoor, A.; Mojoudi, F.; Arjomand, O., Pb(II) removal from synthetic wastewater using kombucha scoby and graphene oxide/Fe_3O_4, *Phys. Chem. Res.* **2018**, *6*, 759-771. DOI: 10.22036/pcr.2018.133392.1490.

[12] Manera, C.; Tonello, A. P.; Perondi, D.; Godinho, M., Adsorption of leather dyes on activated carbon from leather shaving wastes: kinetics, equilibrium and thermodynamics studies. *Environ. Technol.* **2018**, *40*, 2756-2768. DOI: 10.1080/09593330.2018.1452984.

[13] Vimonses, V.; Jin, B.; Chow, C. W. K., Insight into removal kinetic and mechanisms of anionic dye by calcined clay materials and lime. *J. Hazard. Mater.* **2010**, *177*, 420-427. DOI: 10.1016/j.jhazmat.2009.12.049.

[14] Bharathi, K. S.; Ramesh, S. T., Removal of dyes using agricultural waste as low-cost adsorbents: a review. *Appl. Water Sci.* **2013**, *3*, 773-790. DOI: 10.1007/s13201-013-0117-y.

[15] Esmaeili, H.; Foroutan, R., Adsorptive behavior of methylene blue onto sawdust of sour lemon, date

palm, and eucalyptus as agricultural, *J. Dispers. Sci. Technol.* **2018**, *40*, 990-999. DOI: 10.1080/01932691.2018.1489828.

[16] Zare, E. N.; Motahari, A.; Sillanpää, M., Nanoadsorbents based on conducting polymer nanocomposites with main focus on polyaniline and its derivatives for removal of heavy metal ions/dyes: A review. *Environ. Res.* **2018**, *162*, 173-195. DOI: 10.1016/j.envres.2017.12.025.

[17] Gospodinova, N.; Skorokhoda, T.; Lobaz, V., Remarkable ability to modulate light transmittance and block heat in the bleached state combined in one electrochromic material: Highly crystalline polyaniline. *Macromolecules.* **2018**, *51*, 2227-2231. DOI: 10.1021/acs.macromol.7b02543.

[18] Majhi, D.; Patra, B. N., Preferential and enhanced adsorption of dyes on alum doped nanopolyaniline. *J. Chem. Eng. Data.* **2018**, *63*, 3427-3437. DOI: 10.1021/acs.jced.8b00312.

[19] Ayad, M. M.; El-Nasr, A. A., Adsorption of cationic dye (methylene blue) from water using polyaniline nanotubes base. *J. Phys. Chem. C.* **2010**, *114*, 14377-14383. DOI: 10.1021/jp103780w.

[20] Amer, W. A.; Omran, M. M.; Rehab, A. F.; Ayad, M. M., Acid green crystal-based: In situ synthesis of polyaniline hollow nanotubes for the adsorption of anionic and cationic dyes. *RSC Adv.* **2018**, *8*, 22536-22545. DOI: 10.1039/c8ra02236d.

[21] Vural, T.; Yaman, Y. T.; Ozturk, S.; Abaci, S.; Denkbas, E. B., Electrochemical immunoassay for detection of prostate specific antigen based on peptide nanotube-gold nanoparticle- polyaniline immobilized pencil graphite electrode. *J. Colloid Interface Sci.* **2018**, *510*, 318-326. DOI: 10.1016/j.jcis.2017.09.079.

[22] Zhu, J.; Shao, C.; Li, X.; Han, C.; Yang, S.; Ma, J.; Li, X.; Liu, Y., Immobilization of ZnO/polyaniline heterojunction on electrospun polyacrylonitrile nanofibers and enhanced photocatalytic activity. *Mater. Chem. Phys.* **2018**, *214*, 507-515. DOI: 10.1016/j.matchemphys.2018.04.053.

[23] Bahrudin, N. N.; Nawi, M. A.; Izhan, W.; Wan, N., Physical and adsorptive characterizations of immobilized polyaniline for the removal of methyl orange dye. *Korean J. Chem. Eng.* **2018**, *35*, 1-12. DOI: 10.1007/s11814-018-0052-6.

[24] Salian, G. D.; Lebouin, C.; Demoulin, A.; Lepihin, M. S.; Maria, S.; Galeyeva, A. K.; Kurbatov, A. P.; Djenizian, T., Electrodeposition of polymer electrolyte in nanostructured electrodes for enhanced electrochemical performance of thin-film Li-ion microbatteries. *J. Power Sources.* **2017**, *340*, 242-246. DOI: 10.1016/j.jpowsour.2016.11.078.

[25] Lee, J.; Shin, S. J.; Lee, J. G.; Yun, J.; Oh, M.; Chung, T. D., Direct electrodeposition of thin metal films on functionalized dielectric layer and hydrogen gas sensor. *J. Electrochem. Soc.* **2017**, *164*, 1-5. DOI: 10.1149/2.0061702jes.

[26] Mroczka, R.; Rafa, Ł.; Grzegorz, Ż., Molecular analysis of additives and impurities accumulated on copper electrodeposited layer by time-of- fl ight secondary ion mass spectrometry. *Appl. Surf. Sci.* **2019**, *463*, 412-426. DOI: 10.1016/j.apsusc.2018.08.238.

[27] El Jaouhari, A.; Laabd, M.; Aouzal, Z.; Bouabdallaoui, M.; Bazzaoui, E. A.; Albourine, A.; Martins, J. I.; Wang, R.; Bazzaoui, M., Effect of electrolytic conditions on PA electrosynthesis on stainless steel : A new application to polycarboxy-benzoic acids removal from industrial effluents. *Prog. Org. Coatings.* **2016**, *101*, 233-239. DOI: 10.1016/j.porgcoat.2016.06.021.

[28] Kaewsongpol, T.; Sawangphruk, M.; Chiochan, P., High-performance supercapacitor of electrodeposited porous 3D polyaniline nanorods on functionalized carbon fiber paper : Effects of hydrophobic and hydrophilic surfaces of conductive carbon paper substrates. *Mater. Today Commun.* **2015**, *4*, 176-185. DOI: 10.1016/j.mtcomm.2015.08.005.

[29] Zhou, D.; Che, B.; Lu, X., Rapid one-pot electrodeposition of polyaniline/manganese dioxide hybrids: a facile approach to stable high-performance anodic electrochromic materials. *J. Mater. Chem. C.* **2017**, *5*, 1758-1766. DOI: 10.1039/c6tc05216a.

[30] Lu, J. J.; Gu, Y. H.; Chen, Y.; Yan, X.; Guo, Y. J.; Lang, W. Z.; Ultrahigh permeability of graphene-based membranes by adjusting D-spacing with poly (ethylene imine) for the separation of dye wastewater. *Sep. Purif. Technol.* **2019**, *210*, 737-745. DOI:

10.1016/j.seppur.2018.08.065.

[31] Yoon, S. B.; Yoon, E. H.; Kim, K. B., Electrochemical properties of leucoemeraldine, emeraldine, and pernigraniline forms of polyaniline/multi-wall carbon nanotube nanocomposites for supercapacitor applications. *J. Power Sources*. **2011**, *196*, 10791-10797. DOI: 10.1016/j.jpowsour.2011.08.107.

[32] Plesu, N.; Kellenberger, A.; Mihali, M.; Vaszilcsin, N.; Effect of temperature on the electrochemical synthesis and properties of polyaniline films. *J. Non. Cryst. Solids*. **2010**, *356*, 1081-1088. DOI: 10.1016/j.jnoncrysol.2010.01.011.

[33] Xu, P.; Tang, Q.; Chen, H.; He, B., Insights of close contact between polyaniline and FTO substrate for enhanced photovoltaic performances of dye-sensitized solar cells, *Electrochim. Acta*. **2014**, *125*, 163-169. DOI: 10.1016/j.electacta.2014.01.107.

[34] Buron, C. C.; Lakard, B.; Monnin, A. F.; Moutarlier, V.; Lakard, S., Elaboration and characterization of polyaniline films electrodeposited on tin oxides. *Synth. Met.* **2011**, *161*, 2162-2169. DOI: 10.1016/j.synthmet.2011.08.021.

[35] Wang, X.; Li, Y.; Zhao, Y.; Liu, J.; Tang, S.; Feng, W., Synthesis of PA nanostructures with various morphologies from fibers to micromats to disks doped with salicylic acid. *Synth. Met.* **2014**, *160*, 2008-2014. DOI: 10.1016/j.synthmet.2010.07.030.

[36] Haspulat, B.; Gülce, A.; Gülce, H., Efficient photocatalytic decolorization of some textile dyes using Fe ions doped polyaniline film on ITO coated glass substrate, *J. Hazard. Mater.* **2013**, *260*, 518-526. DOI: 10.1016/j.jhazmat.2013.06.011.

[37] Lyu, W.; Yu, M.; Feng, J.; Yan, W., Applied surface science highly crystalline polyaniline nano fibers coating with low-cost biomass for easy separation and high efficient removal of anionic dye ARG from aqueous solution. *Appl. Surf. Sci.* **2018**, *458*, 413-424. DOI: 10.1016/j.apsusc.2018.07.074.

[38] Bhaumik, M.; McCrindle, R. I.; Maity, A.; Agarwal, S.; Gupta, V. K., Polyaniline nanofibers as highly effective re-usable adsorbent for removal of reactive black 5 from aqueous solutions. *J. Colloid Interface Sci.* **2016**, *466*, 442-451. DOI: 10.1016/j.jcis.2015.12.056.

[39] Patra, B. N.; Majhi, D., Removal of anionic dyes from water by potash alum doped polyaniline: Investigation of kinetics and thermodynamic parameters of adsorption. *J. Phys. Chem. B*. **2015**, *119*, 8154-8164. DOI: 10.1021/acs.jpcb.5b00535.

[40] Gemeay, A. H.; El-Sharkawy, R. G.; Mansour, I. A.; Zaki, A. B., Application of polyaniline/manganese dioxide composites for degradation of acid blue 25 by hydrogen peroxide in aqueous media. *Bull. Mater. Sci.* **2012**, *35*, 585-593. DOI: 10.1007/s12034-012-0328-0.

[41] Foroutan, R.; Mohammadi, R.; Farjadfard, S.; Esmaeili, H.; Ramavandi, B.; Sorial, G. A., Eggshell nano-particle potential for methyl violet and mercury ion removal: Surface study and field application, *Adv. Powder Technol.* **2019**, *30*, 2188-2199. DOI: 10.1016/j.apt.2019.06.034.

[42] Foo, K. Y.; Hameed, B. H., Bioresource technology microwave-assisted preparation and adsorption performance of activated carbon from biodiesel industry solid reside : Influence of operational parameters. *Bioresour. Technol.* **2012**, *103*, 398-404. DOI: 10.1016/j.biortech.2011.09.116.

[43] Swenson, H.; Stadie, N. P., Langmuir's theory of adsorption: A centennial review, *Langmuir*. **2019**, *35*, 5409-5426. DOI: 10.1021/acs.langmuir.9b00154.

[44] Tamjidi, S.; Esmaeili, H., Chemically modified CaO/Fe_3O_4 nanocomposite by Sodium dodecyl sulfate for Cr(III) removal from water. *Chem. Eng. Technol.* **2019**, *42*, 607-616. DOI: 10.1002/ceat.201800488.

[45] Maruthapandi, M.; Kumar, V. B.; Luong, A. J. H. T., Gedanken, kinetics, isotherm, and thermodynamic studies of methylene blue adsorption on polyaniline and polypyrrole macro-nanoparticles synthesized by C-Dot-initiated polymerization. *ACS Omega*. **2018**, *3*, 7196-7203. DOI: 10.1021/acsomega.8b00478.

[46] Ahmadi, F.; Esmaeili, H., Chemically modified bentonite/Fe_3O_4 nanocomposite for Pb(II), Cd(II) and Ni(II) removal from synthetic wastewater, *Desalin. Water Treat.* **2018**, *110*, 154-167. DOI: 10.5004/dwt.2018.22228.

[47] Xiong, L.; Yang, Y.; Mai, J.; Sun, W.; Zhang, C.; Wei, D.; Chen, Q.; Ni, J., Adsorption behavior of

methylene blue onto titanate nanotubes. *Chem. Eng. J.* **2010**, *156*, 313-320. DOI: 10.1016/j.cej.2009.10.023.

[48] Yeganeh, G.; Ramavandi, B.; Esmaeili, H.; Sajad, T., Dataset of the aqueous solution and petrochemical wastewater treatment containing ammonia using low cost and ef fi cient bio- adsorbents, *Data Br.* **2019**, *26*, 104308. DOI: 10.1016/j.dib.2019.104308.